Innovative Infrastructure Solutions (2025) 10:403
https://doi.org/10.1007/s41062-025-02173-w

TECHNICAL PAPER

# Geotechnical implications of sand–rubber mixture in transportation infrastructure: assessing shear strength and compressibility characteristics

Mohammad Afrazi[1] · Danial Jahed Armaghani[2] · Hossein Afrazi[3] · Salman Rouhanifar[4] · Hadi Fattahi[5]

Received: 28 March 2024 / Accepted: 5 July 2025


## Abstract

The increase of discarded tires in urban environments has emerged as a pressing environmental concern. This study explores the potential of incorporating scrap tire particles into sand matrices as a sustainable solution to diminish tire stockpiles and decrease environmental pollution. The main focus of this research is to investigate the mechanical properties of loose sand–rubber mixtures (SRM) characterized by a void ratio of 0.86, with varying rubber-to-sand particle size ratios (SR) of 0.25, 1, and 4. An extensive set of 300 direct shear tests was conducted using normal stresses (NS) of 50, 100, and 150 kPa. These tests were supplemented by 110 Oedometer tests using constant NS of 60 kPa for three days, 60 kPa for 1.5 days with an additional 140 kPa for 1.5 days, and 200 kPa for three days. Analysis of shear stress and deformation characteristics reveals that mixtures with different size ratios show similar trends but different values, which means characteristics of SRM depend not only on rubber content but also on size ratio. The addition of rubber particles to the mixtures makes the material more deformable and alters its softening behaviour. Specifically, adding up to 20% rubber content increases the mixture's friction angle, while higher rubber percentages cause it to decrease. A critical transition point is identified at approximately 20% rubber content, where the sand component begins to mimic rubber behaviour. Additionally, mixtures with SR = 0.25 exhibited a lower dilation angle compared to those with higher SR values, indicating that smaller rubber particles contribute to reduced dilation. Furthermore, the compressibility tendency of SRM escalates with higher rubber proportions, with mixtures featuring an SR of 0.25 exhibiting the most pronounced compressibility under equivalent NS conditions.

**Keywords** Scrap tire recycling · Sustainable materials · Shear strength · Deformation behaviour · Oedometer testing · Particle size ratio

## List of symbols

| | |
|---|---|
| SRM | Sand–rubber mixtures |
| NS | Normal stress |
| SR | Size ratio (rubber-to-sand particle size ratio) |
| FR | Rubber fraction ($\frac{V_R}{V_R+V_S}$) |
| PSD | Particle size distribution |
| kPa | Kilopascal |
| SRC | Sand–rubber composites |
| $D_R$ | Diameter of rubber particles |
| $D_S$ | Diameter of sand particles |
| SF | Sand fraction |
| $G_s$ | Specific gravity |

✉ Danial Jahed Armaghani
danial.jahedarmaghani@uts.edu.au

Mohammad Afrazi
Mohammad.afrazi@student.nmt.edu

Hossein Afrazi
hosseinafrazi0@gmail.com

Salman Rouhanifar
Salman.rouhanifar@modares.ac.ir

Hadi Fattahi
h.fattahi@arakut.ac.ir

[1] Mechanical Engineering Department, New Mexico Institute of Mining and Technology, Socorro, NM 87801, USA

[2] School of Civil and Environmental Engineering, University of Technology Sydney, Sydney, NSW 2007, Australia

[3] Department of Civil, Water and Environmental Engineering, Shahid Bahonar University of Kerman, Kerman, Iran

[4] School of Civil and Environmental Engineering, Tarbiat Modares University, Tehran, Iran

[5] Faculty of Earth Sciences Engineering, Arak University of Technology, Arak, Iran

Published online: 14 August 2025

| | |
|---|---|
| $C_u$ | Uniformity coefficient |
| $C_c$ | Gradation coefficient |
| $D_{10}, D_{30}$, and $D_{60}$ | Diameter below which 10, 30, and 60% of the particles, by weight, are found respectively |

## Introduction

The utilization of unconventional materials in geotechnical engineering has gained significant attention in recent years as researchers and engineers seek innovative solutions to address environmental challenges associated with waste disposal and the optimization of construction materials [1–9]. Among these unconventional materials, the combination of sand and rubber has emerged as a promising path, presenting a unique mixture of sustainable resource management and improved geotechnical performance [10–15]. The integration of rubber particles, derived from discarded tires, into sand matrices has opened new possibilities for enhancing the properties and applications of geotechnical materials [16–21].

The accumulation of discarded tires worldwide has become a growing concern, posing significant environmental and economic challenges due to their non-biodegradable nature and slow decomposition rates [22–24]. Traditional methods of tire disposal, such as landfilling and stockpiling, have proven to have negative impact on ecosystems and economically burdensome. In response to this issue, researchers and engineers have turned to the repurposing of scrap tires as a valuable resource in geotechnical engineering [25–30].

This innovative approach involves the incorporation of rubber particles into sand-based mixtures, resulting in sand–rubber composites (SRC) that exhibit unique mechanical, hydraulic, and environmental properties [31–36]. The combination of these materials has shown promise in various geotechnical applications, ranging from enhancing the stability of embankments and retaining walls to improving drainage systems and reducing settlement [37–44]. Understanding sand–rubber mixtures (SRM)'s performance and behaviour is essential to realizing its full potential for sustainable geotechnical engineering practices. Waste tire use, either in its totality or in processed forms, has become more common in the fields of civil and geotechnical engineering in recent years. This trend can be attributed to various advantageous properties inherent in rubber particles, including their lightweight nature, high elasticity, capacity to absorb vibrations, excellent hydraulic characteristics, low lateral pressure, and effective temperature insulation [45–52]. Kawata et al. [53] recommended the incorporation of rubber particles in civil engineering applications because of their light weight and elastic deformation. Additionally, Garga and O'Shaughnessy [54] and O'Shaughnessy and Garga [55] successfully employed non-processed scrap tires to improve the construction of retaining walls and slopes. The utilization of discarded tires for slope stabilization has been demonstrated to be both economically and technically beneficial, as illustrated by Poh and Broms [56]. Furthermore, Huat et al. [57] employed whole scrap tires to rehabilitate tropical soil slopes. Notably, tire-reinforced embankment structures have displayed enhanced strength and reduced settling when compared to their non-reinforced counterparts [58–62]. Investigating the performance of SRM becomes imperative when addressing the aforementioned challenges. To accomplish this task, many laboratory experiments have been done to analyze the mechanical characteristics of SRM. These investigations encompassed the utilization of Triaxial testing [63–65], direct shear testing, and oedometer [13, 66] testing methodologies. In general, several parameters, including density, rubber forms and sizes, rubber content, form variations between rubber and soil particles, and the size ratio between rubber and sand particles ($D_R/D_S$), affect SRM's mechanical performances. The variables $D_R$ and $D_S$ stands for, respectively, average sand and rubber particle sizes. Up to this date, some researches have been done to investigate the effect of $D_R/D_S$ in SRMs.

Youwai and Bergado [67] carried out triaxial experiments at varied confining pressures of 50, 100, and 200 kilo Pascal with $\frac{D_R}{D_S}$ of around 10. Their goal was to investigate the shear stress and deformation properties of SRM. The mixtures were prepared using cubical rubber grains, and different rubber percentage were incorporated, ranging from 0 to 100%. It was observed that increasing rubber content within the mixtures, there was a corresponding decrease in the maximum shear stress of the SRM, while the shear strain at peak load increased. For instance, in comparison to a mixture devoid of rubber (0% rubber), a mixture containing 50% rubber exhibited a greater peak shear stress but a lower displacement at the point of maximum shear stress. In order to study the mechanical behaviour of SRM with $D_R$ to $D_S$ of 0.25 under an 80 kPa confining pressure, Lee et al. [1] employed triaxial laboratory experiments. Their results showed, the peak strength decreases for mixtures with a lower sand fraction (SF), followed by an increase in the axial strain at peak strength, and no peak strength is also visible for mixtures with a lower SF of 0.6, according to tests with various SF of 0, 0.2, 0.4, 0.6, 0.7, 0.8, 0.9, and 1. Large-scale direct shear experimental tests on sand with tire chips were performed by Takano et al. [68]. They discovered that the tire aspect ratio and content had an impact on the mixes' shear strength values. Additionally, they found that sand reinforced with shreds has more angle friction than pure sand tests. Liu et al. [69] investigated effects of particle size ratio on the shear strength of SRM under normal cyclic loading. Their results showed SRM with larger rubber particles

have higher shear strength compare to the same rubber content but smaller rubber particles. Boominathan and Banerjee [70] conducted experimental tests on different FRs and they showed increasing rubber content will decrease shear strength of the mixtures.

According to research findings, the presence of rubber grains inside SRM affects how the mixtures deform [13, 71–75]. Neaz Sheikh et al. [76] performed a one-dimensional compression test on SRM with NS of up to 745 kPa and then unloaded to 38 kPa. By increasing the rubber percentages in the composite, the compressibility behaviour of the SRM enhanced which is obvious according to inherit flexibility of rubbers. Oedometer laboratory tests were performed by Lee et al. [1] utilizing different SF up to the effective stress of 556 kPa on SRM where $D_R$ to $D_S$ was 0.25. Their results showed, by increasing the SF of SRM, the vertical strain of composite is reduced. Additionally, they demonstrated that in all three confinements, modulus and shear modulus increases when the SF is increased (or rubber volume are decreased). Oedometer experiments were performed by Huat et al. [57] on SRM with $D_R$ to $D_S$ of 10 and various rubber portions. They concluded that compression and swelling rise as the rubber volume of the composite increases. Boominathan and Banerjee [70] investigated the effect of rubber content on the deformability of SRM and demonstrated that with increasing the FR the compressibility of the mixtures will decreases.

As it was shown, the mechanical behaviour of SRM are affected by several parameters. As mentioned, there are lots of researches in the literature, studying sand–rubber behaviour but the effect of $D_R$ to $D_S$, has not received enough attention. The research presented in this study represents a new exploration of how varying $D_R$ to $D_S$ impacts the mechanical properties of SRM. In the previous study of the same research group [3], the authors have investigated only the shear behaviour of materials by conducting direct shear tests. However, to understand the long term behaviour of SRM in this study the authors studied the compression and consolidation behaviour of SRM. Specifically, this study examine scenarios where rubber particles are four times smaller as well as four times larger than sand particles, while maintaining the same particle size distribution (PSD). These investigations are conducted under conditions of low compaction effort and with different rubber volume fractions, using direct shear and oedometer tests. Since in this study sand grains and rubber particles have the same PSD the only affecting factor will be the texture and inherit characteristics of materials.

## Materials and methodology

### Sand

Rubber was combined with Firoozkooh Sand Fraction 131 to create the composite. To get the desired grain size distribution, which ranged from 0.3 to 1 mm, the sand particles underwent sifting, as shown in Fig. 1. Figure 2 shows that the sand particles are primarily angular to sub-angular in form. The modified Firoozkooh sand fraction

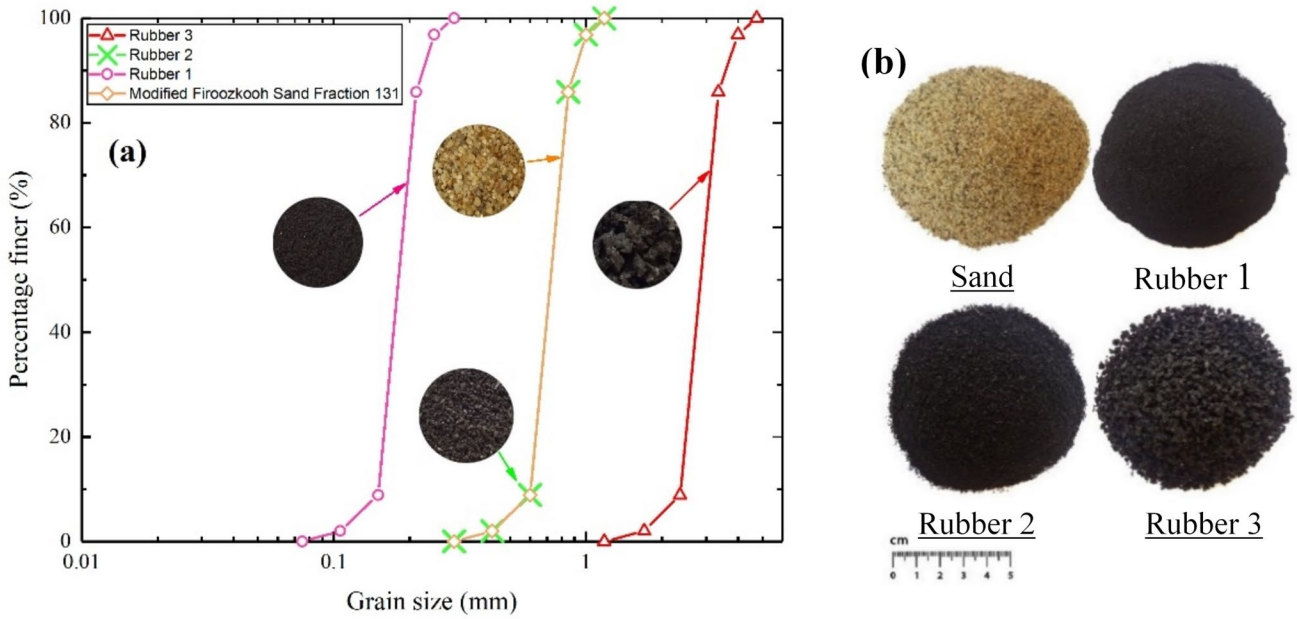


**Fig. 1** **a** Used material PSD. **b** Sand and of rubber types

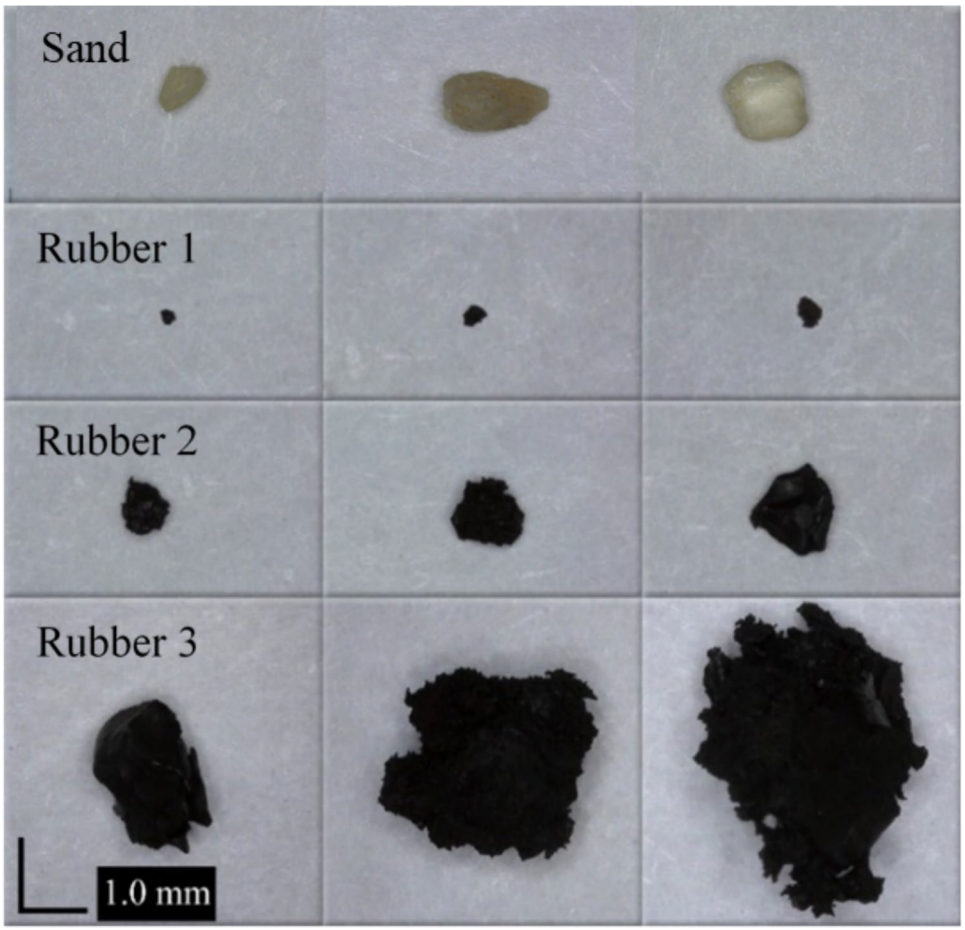


**Fig. 2** Macroscopic pictures of the used particles

131 specifies void ratios of 0.59 at the minimum and 0.97 at the maximum, respectively, as per the British specification BS1377-4:1990. The table below lists further sand-specific characteristics.

## Rubber

The same rubber material was accurately combined with sand particles, resulting in the generation of three distinct particle size distributions. As visually represented in Fig. 1, the rubber particles underwent a rigorous sieving process to attain size distributions that exhibited three specific relationships to the sand particles: some were four times smaller, some were identical in size, and some were four times larger than the sand particles. This careful manipulation of particle sizes allowed for a comprehensive examination of the effects of varying particle size ratios on the subsequent mixtures.

Moreover, to facilitate a deeper understanding of the materials used, Table 1 offers a comprehensive breakdown of the key properties and characteristics associated with the rubber, serving as a valuable reference point for the subsequent analyses.

**Table 1** Characteristics of the materials [3]

| Properties | Sand | Rubber 1 | Rubber 2 | Rubber 3 |
|---|---|---|---|---|
| Maximum void ration | 0.97 | – | – | – |
| Minimum void ration | 0.59 | – | – | – |
| $G_s$ | 2.65 | 1.04 | 1.04 | 1.04 |
| $C_u$* | 1.26 | 1.26 | 1.26 | 1.26 |
| $C_c$** | 0.95 | 0.95 | 0.95 | 0.95 |

$^{*}C_u = \frac{D_{60}}{D_{10}}$

$^{**}C_c = \frac{D_{30}^2}{D_{60}D_{10}}$

## Sample preparation of direct shear test

In this study, sand–rubber composite specimens with varying rubber volume fractions were subjected to direct shear testing, as shown in Fig. 3, at a constant speed of 0.5 mm/min. The specimens were prepared in a shear box with dimensions of 100 mm × 100 mm and a height of 35 mm. To ensure homogeneity and prevent the potential segregation of ingredients during laboratory testing, it was essential that well-mixed samples were created.

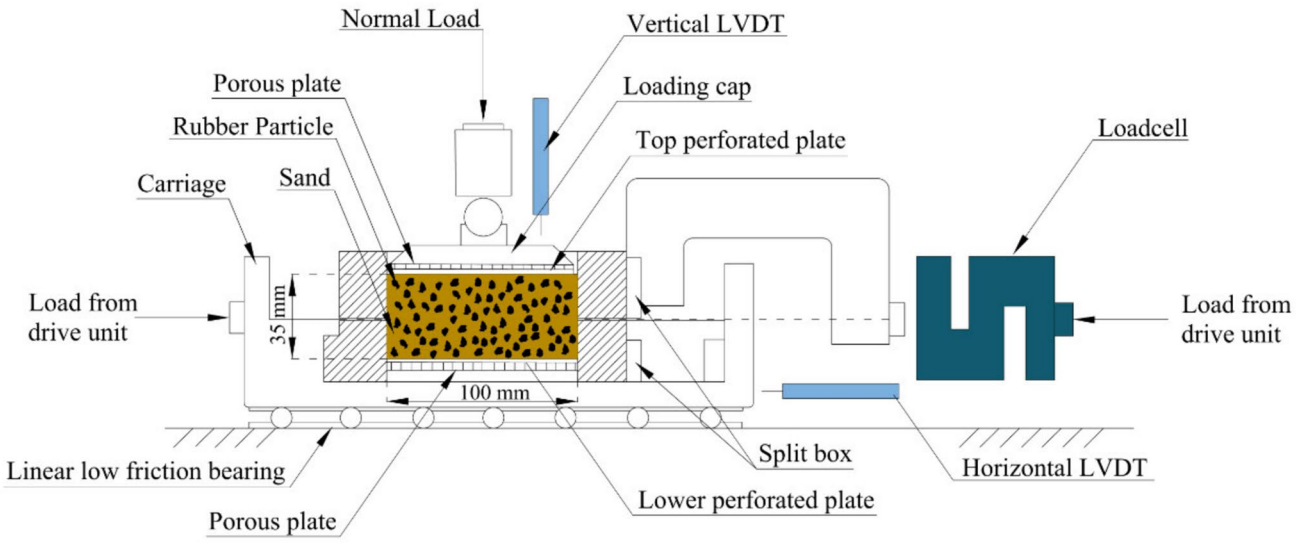


**Fig. 3** Schematic diagram of direct shear test

To achieve this, the moist tamping method was employed, a widely recognized technique for producing uniform mixtures in laboratory settings [3, 77–80]. The process began with the mixing of sand and rubber particles in a circular bowl. To ensure that all particles were adequately coated and evenly distributed, 10% water by volume was added. This water content was carefully measured to ensure that the particles remained slightly damp, which facilitated a uniform mixture without causing clumping. Once the mixture was prepared, it was spoon-deposited into the shear box in three successive layers. The zero height drop technique was used to place each layer carefully, minimizing the risk of particle segregation [81]. Each layer was then lightly tamped to achieve a uniform relative density of 30%, ensuring consistency across all samples [82].

Three different rubber volume fractions were utilized in the mixtures, corresponding to $D_R$ to $D_S$ ratios of 0.25 (Mixture-1), 1 (Mixture-2), and 4 (Mixture-3). For an assumed rubber fraction ($F_R = \frac{V_R}{V_R+V_S}$) and the fact that all specimens had a void ratio of 0.86, the required masses of sand and rubber in the mixture were calculated.

### Sample preparation of oedometer test

In the oedometer test, as shown in Fig. 4, the mechanical behaviour of sand–rubber mixtures under one-dimensional compression was examined. The specimens were prepared using oedometer cylinders with a height of 50 mm and a diameter of 50 mm. The same moist tamping technique described for the direct shear test was employed to ensure the homogeneity and integrity of the samples.

The sand and rubber particles were first mixed with 10% water to achieve an even distribution. The mixture was then placed into the oedometer cylinder in three layers. Each layer was carefully tamped to ensure that the desired void ratio was achieved consistently across the sample.

Various rubber volume contents—5%, 15%, 25%, and 40%—were used in the oedometer tests, with $D_R$ to $D_S$ ratios of 0.25, 1, and 4 being considered.

## Results and discussion

### Repeatability

To ensure the accuracy and consistency of the findings in this study, each sample underwent four direct shear tests and three oedometer tests and all conducted under meticulously controlled and the same conditions. To ensure the repeatability of results, more than 300 direct shear tests and 110 one-dimensional compression tests were carried out using this information along with the application of nine different rubber fractions for direct shear tests and four different rubber fractions for oedometer tests, three different $D_R$ to $D_S$ values, and three different NS of 50, 100, and 150 kPa for direct shear tests and three NS patterns of 60 kPa, 60 + 140 kPa, and 200 kPa for oedometer tests. In direct shear and oedometer testing with SR = 0.25, Fig. 5 depicts the shear and compression behaviour of SRM in direct shear and oedometer tests. The results nicely repeated, as seen in Fig. 5. The results are thus reported in the next sections of the study, using the averaged data.

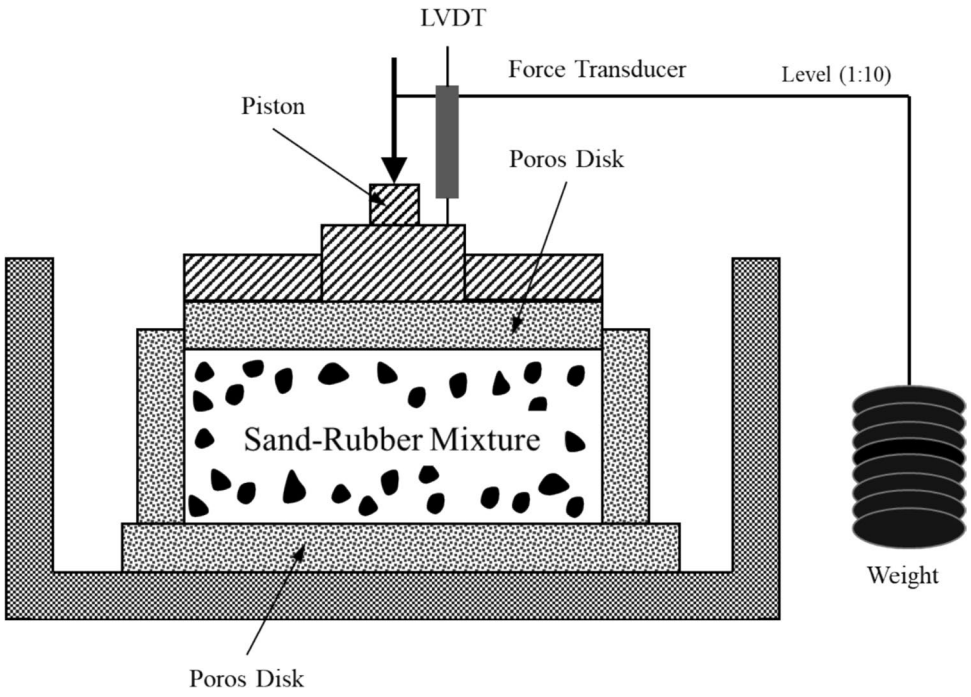


**Fig. 4** Schematic diagram of oedometer test

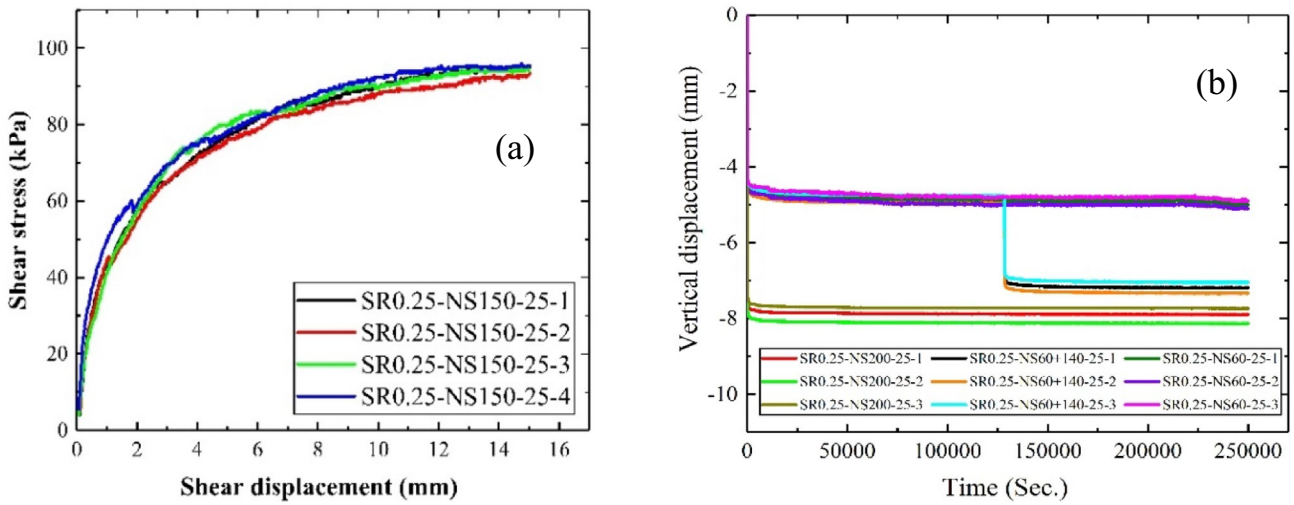


**Fig. 5** **a** Shear stress versus shear displacement under NS of 150 kPa; **b** vertical displacement versus Time of SRM under 150 kPa NS when SR = 0.25

## Shear strength of SRM

Figure 6 provides a visual representation of the shear strength characteristics exhibited by SRM under varying $D_R$ to $D_S$ values and different rubber content percentages, specifically 10%, 20%, 30%, and 40%. Notably, the figure illustrates a distinct pattern: in comparison to mixtures featuring $D_R$ to $D_S$ (size ration, SR) = 0.25, the sand–rubber combinations with SR values of 1 and 4 display notably higher shear strengths. This observation underscores the profound influence of fine rubber particles on particle interactions within the mixtures. In cases where $D_R$ to $D_S$ = 0.25, the presence of fine rubber particles results in a dominance of rubber-to-rubber interactions, as these particles envelop the sand particles. However, as the rubber content increases, especially beyond the 20% threshold, this behaviour assumes greater significance. Consequently, the behaviour of the mixtures begins to resemble that of rubber rather than sand, emphasizing the evolving role of rubber content in shaping the material's mechanical response. It is observed that

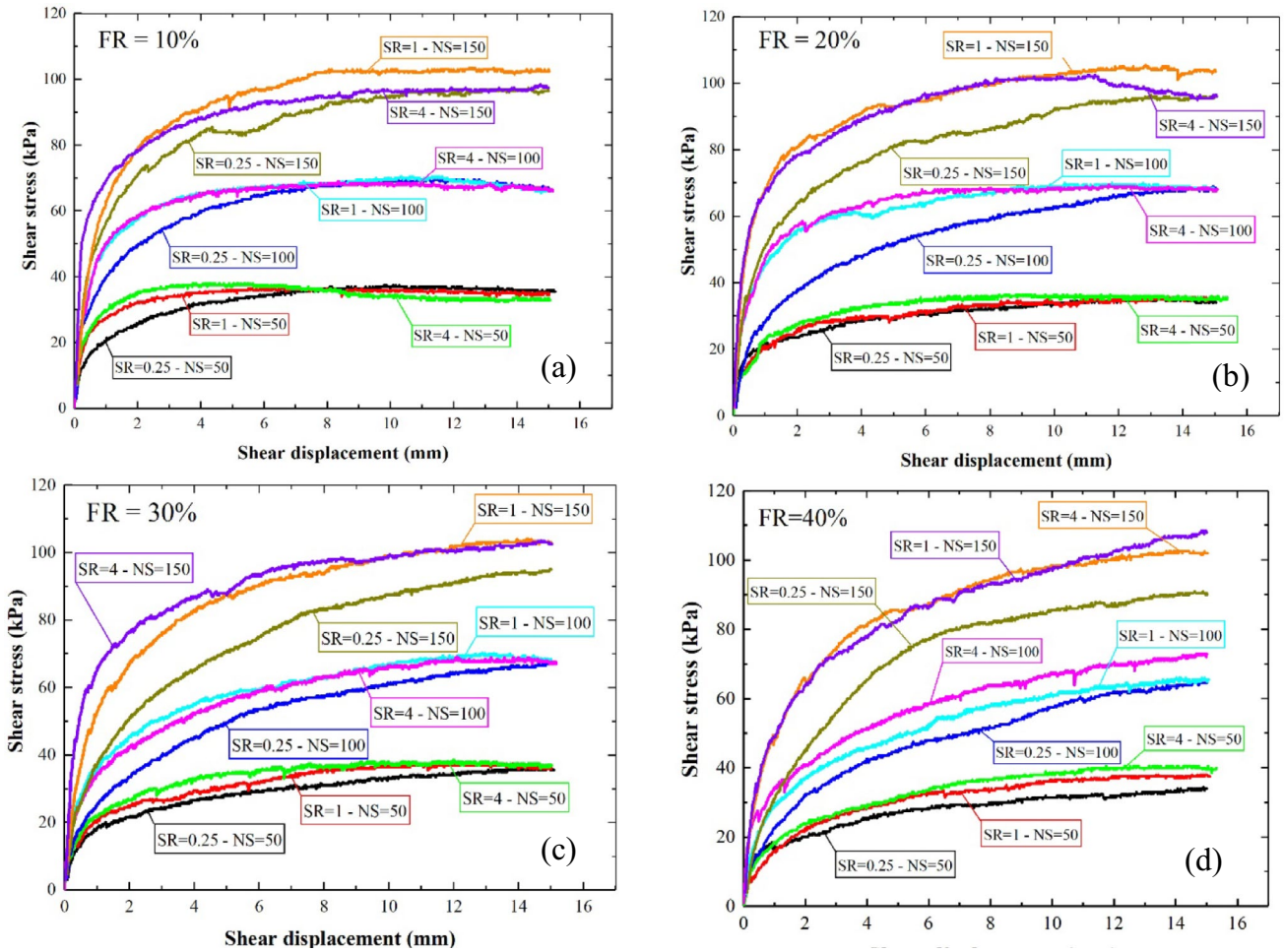


**Fig. 6** Shear stress pattern of SRM under various NS for the rubber content of: **a** 10 percent; **b** 20 percent; **c** 30 percent; **d** 40 percent.

the shear displacement corresponding to the shear strength increases with a higher rubber content in the mixture. It is also worth mentioning that the effect of rubber percentage on shear displacement is more pronounced under normal stresses of 100 kPa and 150 kPa.

The peak shear stress was selected based on the following criterion: if the highest shear stress was attained before a 10 percent displacement of the box, it was chosen. However, if the highest shear stress was not reached before 10 percent displacement, the stress recorded at the 10 percent displacement of the direct shear box length was selected. Figure 7 offers a comparative analysis of the peak shear stress observed in each SRM. The data portrayed in the figure reveals a notable trend: when the FR exceeds 20%, the peak shear stress in mixtures with SR greater than 1 surpasses that in mixtures with SR values less than 1. Interestingly, it becomes apparent that the size of the rubber particles exerts minimal influence on FR values below the 20% threshold. In SRMs featuring less than 20% rubber content, sand emerges as the dominant factor influencing their

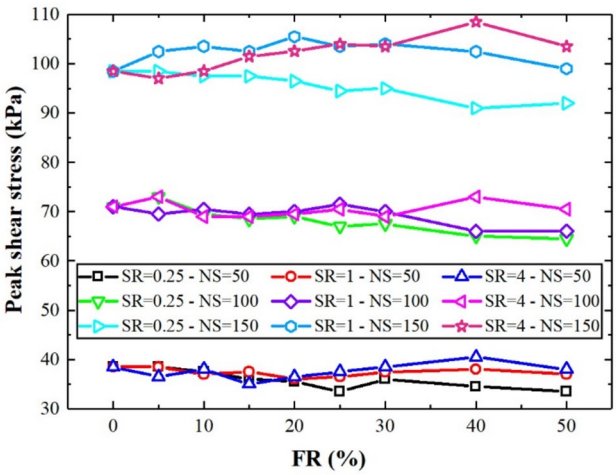


**Fig. 7** Impact of FR on peak shear stress of SRM

mechanical behaviour. On the other hand, the significance of rubber's part becomes more apparent as the rubber content rises over 20%. Additionally, the mechanical behaviour of these mixtures exhibits sensitivity to the size of the rubber particles. Remarkably, these findings align with those previously reported by Takano et al. [68], reinforcing the consistency of these observed trends in the broader context of materials science. However, this finding appears to contradict the research conducted by Youwai and Bergado [67]. Their research showed that the maximum shear strength of SRM decreased as the rubber content increased. This disparity in results could potentially arise from variations in sample density, differences in sample processing methodologies, or variations in SR. It's important to emphasize that the findings reported here remain consistent within the specific context of this investigation, where a void ratio of 0.86 and a relative density of 30 percent were employed. To gain a more comprehensive understanding of these observations and to account for potential variations, further research should explore the impact of different relative densities on the mechanical behaviour of these mixtures [3].

Figure 8 presents the data relating to the friction angle and cohesiveness values across different FR levels. The relationship observed between the friction angle and RF is particularly noteworthy. Notably, regardless of the SR value, the friction angle reaches its highest point in mixtures containing a 20% RF. It is also evident from the Fig. 8, SR of 4 can provide the highest friction angle which can be because of the big edges of rubber particles in SR = 4 mixtures. These findings are intriguing and align with previous research conducted by Rouhanifar and Ibraim [77], especially in cases where samples exhibit higher rubber percentages exceeding 25%. It is also consistent with the findings of [69], who assessed the shear strength of SRM under normal cyclic loading and observed that mixtures containing larger rubber particles exhibited higher shear strength. This parallel with prior research underscores the consistency of these observations and their potential significance in understanding the mechanical behaviour of these mixtures [3].

However, it is worth noting that, in contrast to previous findings, SRM containing a rubber proportion between 20 and 25% exhibited the lowest levels of cohesiveness. This deviation from prior observations suggests that other factors may be at play. One possible reason for the decrease in cohesion might be linked to the suction forces within the blend and the way the particles interlock with each other. Taking a closer look at Fig. 8a, it becomes apparent that mixtures with SR of 0.25 exhibit lower friction angles compared to combinations with higher SR values. Conversely, mixtures with an SR of 4 display higher friction angles than specimens with no rubber content. These trends align with findings from extensive research on sand containing tire chips, as documented by Takano et al. [68], further reinforcing the validity and relevance of these observations in the broader context of materials science.

An interesting trend emerges as the rubber content in SRM increases; the shear displacement of SRM shows a corresponding increase at a given shear force. This pattern aligns with previous research, including studies conducted by Youwai and Bergado [67]. This occurrence can, to some extent, be ascribed to the unique attributes of rubber particles. Rubber particles have a low modulus, a high capacity for deformation, exceptional elasticity, and demonstrate volume incompressibility, specifically, with a rubber Poisson's ratio of around 0.5 [81]. These properties collectively contribute to the observed behaviour, although it's worth noting that the shape of the rubber particles can also be easily changed. In contrast, sand particles may be perceived

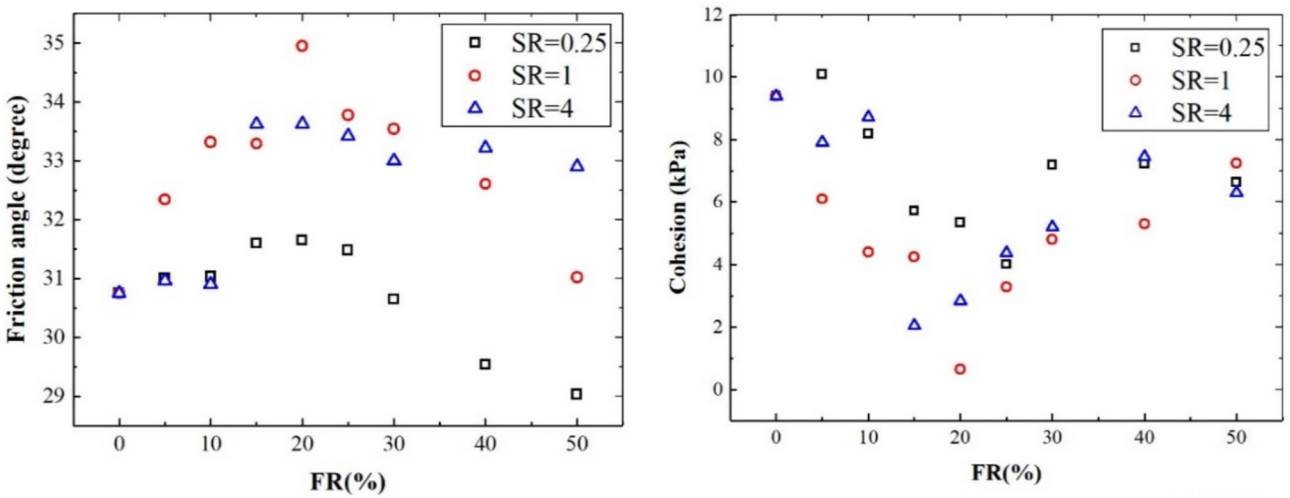


**Fig. 8** **a** Angle of friction and **b** cohesiveness of the SRM with various SR vary in terms of RF

as rigid, given their resistance to compression and limited capacity to change shape. The force dynamics following the mixing of these materials vary, contingent on their respective gradation properties and the mixing ratio [83]. Within this framework, three distinct types of force chains emerge: sand–sand, rubber–rubber, and rubber–sand. When subjected to an external load, the predominant force transmission path is determined by the sand–sand force chain. Consequently, the stress–strain properties of the sand particles dominate the overall behaviour, as evident in Fig. 9. At lower proportions of rubber, the rubber grains are positioned between the sand grains without making direct contact with one another. In contrast, at higher rubber fractions, the rubber particles begin to interact and occupy spaces between sand particles. This shift in particle interaction, coupled with the unique properties of rubber-like particles, leads to the emergence of the rubber–sand–rubber and rubber–rubber force chains as primary routes for transmitting the force. Consequently, the overall stiffness of the rubber–sand mixture experiences a significant reduction [83]. The concept of force chains, as identified in this study, refers to the paths or networks along which forces are transmitted within the material mixture. These force chains, namely sand–sand, rubber–rubber, and rubber–sand, play a crucial role in determining the overall mechanical behaviour of the rubber–sand mixture under external loads. Understanding force chains is crucial in engineering scenarios where materials with different properties are combined. This knowledge can help in predicting how a material will respond to external loads and can be applied in the design of structures and foundations.

The shear displacement behaviour of the mixtures at the shear stress of 60 kPa is visualized in Fig. 10(a). Notably,

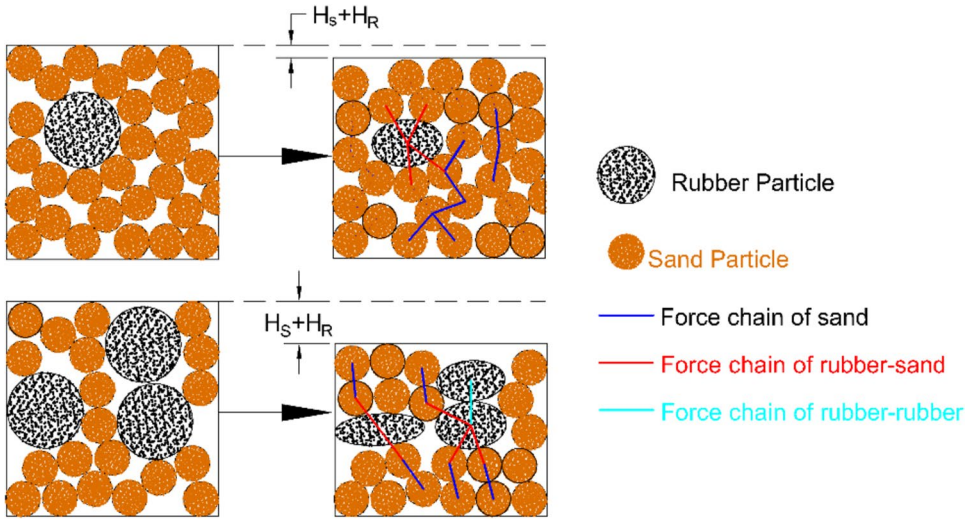


**Fig. 9** Graphic view of displacement of loading SRM

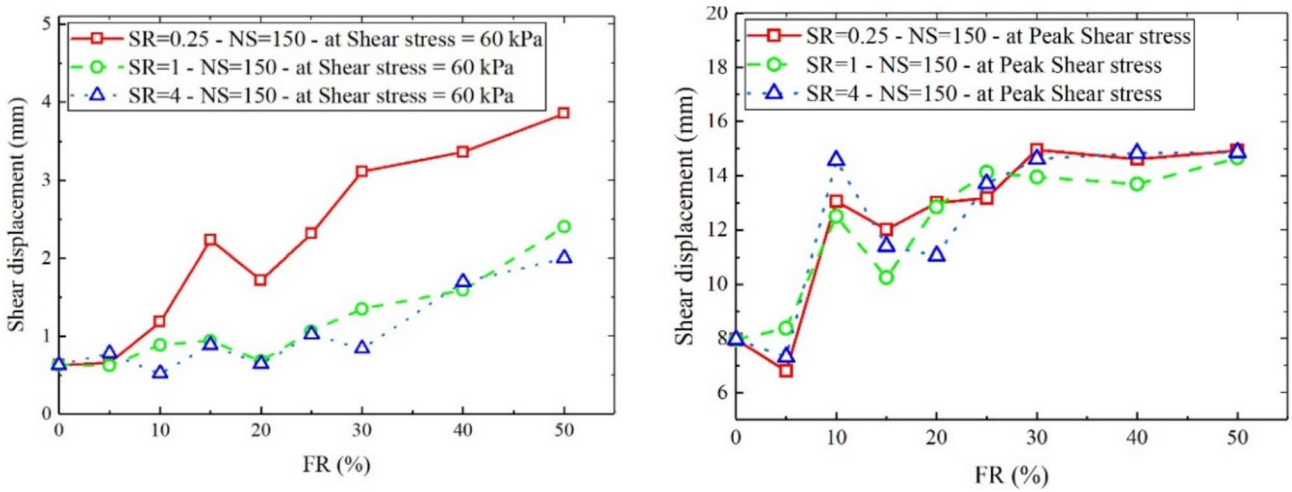


**Fig. 10** Shear displacement of the SRM at shear stresses of **a** 60 kPa and **b** maximum. For all points, NS = 150 kPa

it becomes evident that SRM with the SR of 0.25 exhibit higher shear displacement compared to mixtures featuring higher SR values. This trend suggests that the presence of small rubber particles, which have the ability to envelop sand particles and induce greater material deformation, may be a contributing factor to this observed outcome. Turning to Fig. 10(b), which showcases the shear displacements at the maximum shear stresses, a different pattern emerges. Here, it appears that the SR value does not exert a consistent or systematic influence on the horizontal displacement at the peak stress. This observation underscores the complexity of the mechanical behaviour of these mixtures, which is influenced by various factors beyond just the SR value.

In summary, the findings presented in this section confirm the earlier observations that SRM with varying SR values exhibit diverse shear behaviours. However, it can be concluded that mixtures featuring SR values greater than 1 demonstrate higher shear strength, underscoring their structural integrity, while those with SR values less than 1 exhibit greater ductility, indicating a more flexible response to shear forces.

## Dilation behaviour of SRM

The vertical displacement data for SRM with SR (sand-to-rubber ratio) values of 0.25, 1, and 4 is illustrated in Fig. 11. Analysis of the deformation characteristics of these mixtures reveals a diminishing tendency for dilation as the proportion of rubber in the mixtures increases. This observed trend may be attributed to the compressive behaviour exhibited by rubber particles within the mixtures. The compressibility of the mixtures becomes notably significant when the FR exceeds or equals 20%, indicating that the overall dilation behaviour of SRM is governed by the presence of rubber particles [3].

Numerical studies have also corroborated the influence of rubber particles on the deformation of SRM. For instance, Evans and Valdes [84], utilizing discrete element numerical modelling, determined that the force chain configuration and porosity evolution in the mixture are controlled by the mixing fraction and size ratio of particles. This micromechanical perspective on the subject has been explored by Perez et al. [85] as well.

To gain a deeper understanding of the dilation behaviour of sand–rubber mixtures in this study, the dilation angle for these materials was calculated. As illustrated in Fig. 12, mixtures containing smaller rubber particles ($SR = 0.25$) exhibited a lower dilation angle compared to those with larger rubber particles ($SR = 1and4$), across all normal stress levels. This observation aligns with the general principle that materials with a higher friction angle tend to exhibit greater dilatancy under shear [86, 87]. It is also worth mentioning that the mixtures under higher normal stresses demonstrated lower normal stress which is expected.

## Oedometer tests

Oedometer tests are crucial in the assessment of SRM due to their ability to explain the mechanical behaviour and deformation characteristics of these composite materials [88]. By subjecting the mixture to incremental vertical loads, the sand and rubber components interact and respond under various stress conditions and subsequently deform, Fig. 13 [89]. This is particularly important in the context of sustainable construction and geotechnical engineering, as SRM are often employed in projects aiming to withstand a constant weight. This section, investigate the deformation of SRMs in oedometer tests.

To explore the vertical deformation characteristics of SRM, oedometer tests were employed as part of this investigation. The study encompassed the utilization of three distinct SR and three different NS applied at 60 kPa (over a period of three days), 60 + 140 kPa (distributed as 1.5 days followed by another 1.5 days), and 200 kPa (for a total duration of three days). The chosen normal stress range of 60–140 kPa for the oedometer tests reflects the anticipated pressures in real-world scenarios for the loose material under study. With 60 kPa representing near-surface conditions and 200 kPa corresponding to depths of 3–4 m, the range allows us to explore the material's behaviour under varying stress levels. The results of these experiments are presented in the subsequent figures for analysis and interpretation (Figs. 14, 15, 16).

The figures provided above offer valuable insights into the behaviour of composites under varying loading conditions. Notably, when subjected to an instantaneous loading of 200 kPa, these composites exhibit more pronounced deformation, indicating the significant influence of the applied load. Conversely, composites subjected to an instantaneous loading of 60 kPa display lower levels of deformation, underscoring the importance of the loading magnitude as a critical variable in the deformation response.

Regarding the role of SR, the observations suggest a noteworthy trend. In the majority of cases, composites with an SR of 0.25 tend to exhibit greater levels of deformation. The results of this section is consistent with [70] which showed increasing the rubber content will increase the deformability of the mixtures. This consistent pattern highlights the influence of SR as a contributing factor in the deformation behaviour of these materials.

In this study, it's important to note that the Poisson's ratio was not directly calculated after the adding of rubber into the sand mixture. Instead, an upper constraint of 0.3 and a lower constraint of 0.2 for the Poisson's ratio were assumed based on [90] for the purposes of analysis. Subsequently, the elastic modulus of the mixtures was computed based on these assumed Poisson's ratio values. The following figure illustrates the variation in the elastic modulus

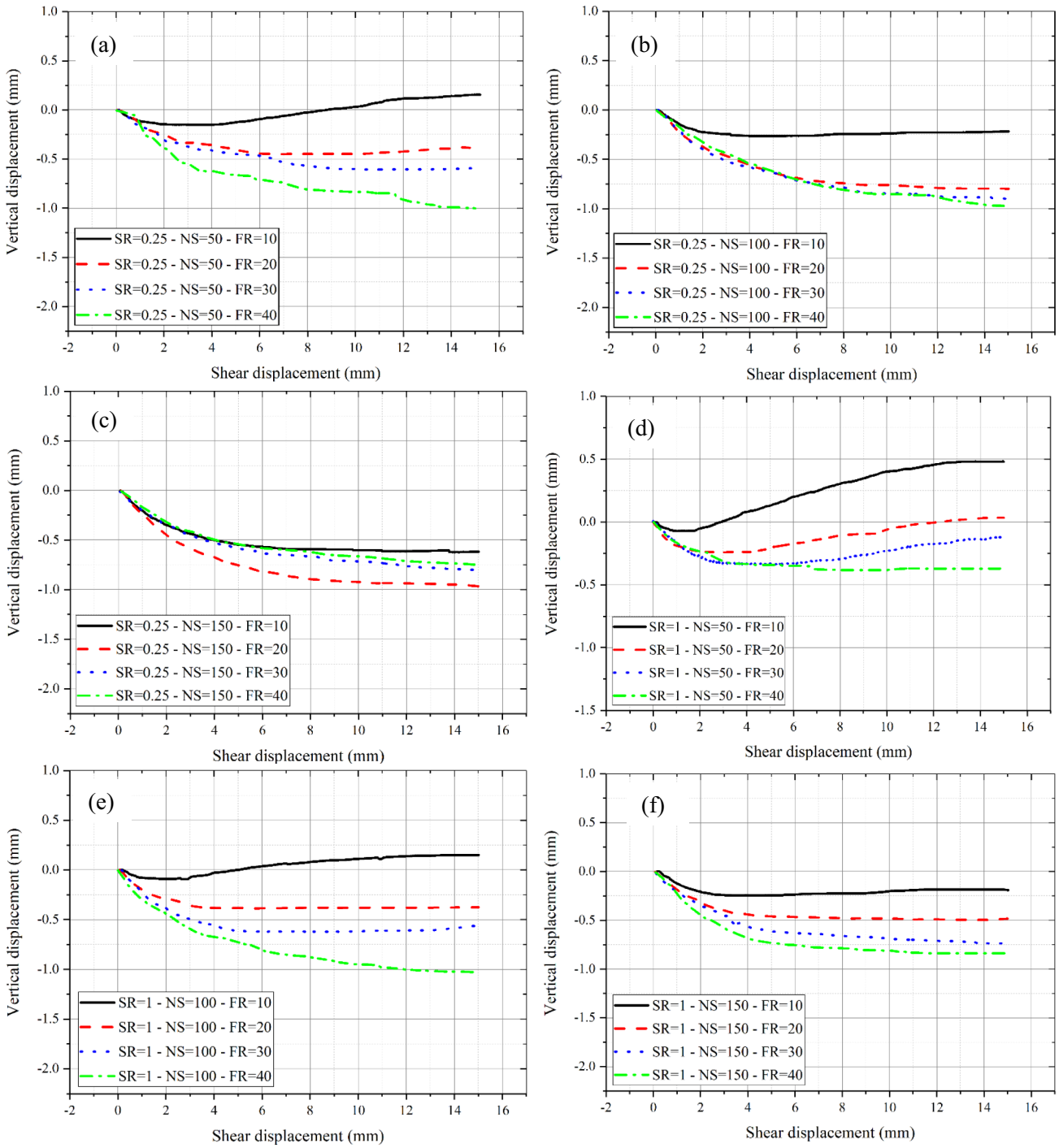


**Fig. 11** Vertical displacement versus shear displacement: **a** SR = 0.25 and NS = 50 kPa; **b** SR = 0.25 and NS = 100 kPa; **c** SR = 0.25 and NS = 150 kPa; **d** SR = 1 and NS = 50 kPa; **e** SR = 1 and NS = 100 kPa; **f** SR = 1 and NS = 150 kPa; **g** SR = 4 and NS = 50 kPa; **h** SR = 4 and NS = 100 kPa; and **i** SR = 4 and NS = 150 kPa

of the SRM. Notably, the figure demonstrates a consistent trend: as more rubber is incorporated into the mixtures, there is a noticeable decrease in the elastic modulus of the SRM. This trend highlights the influence of rubber portion on the stiffness and elasticity of the composite

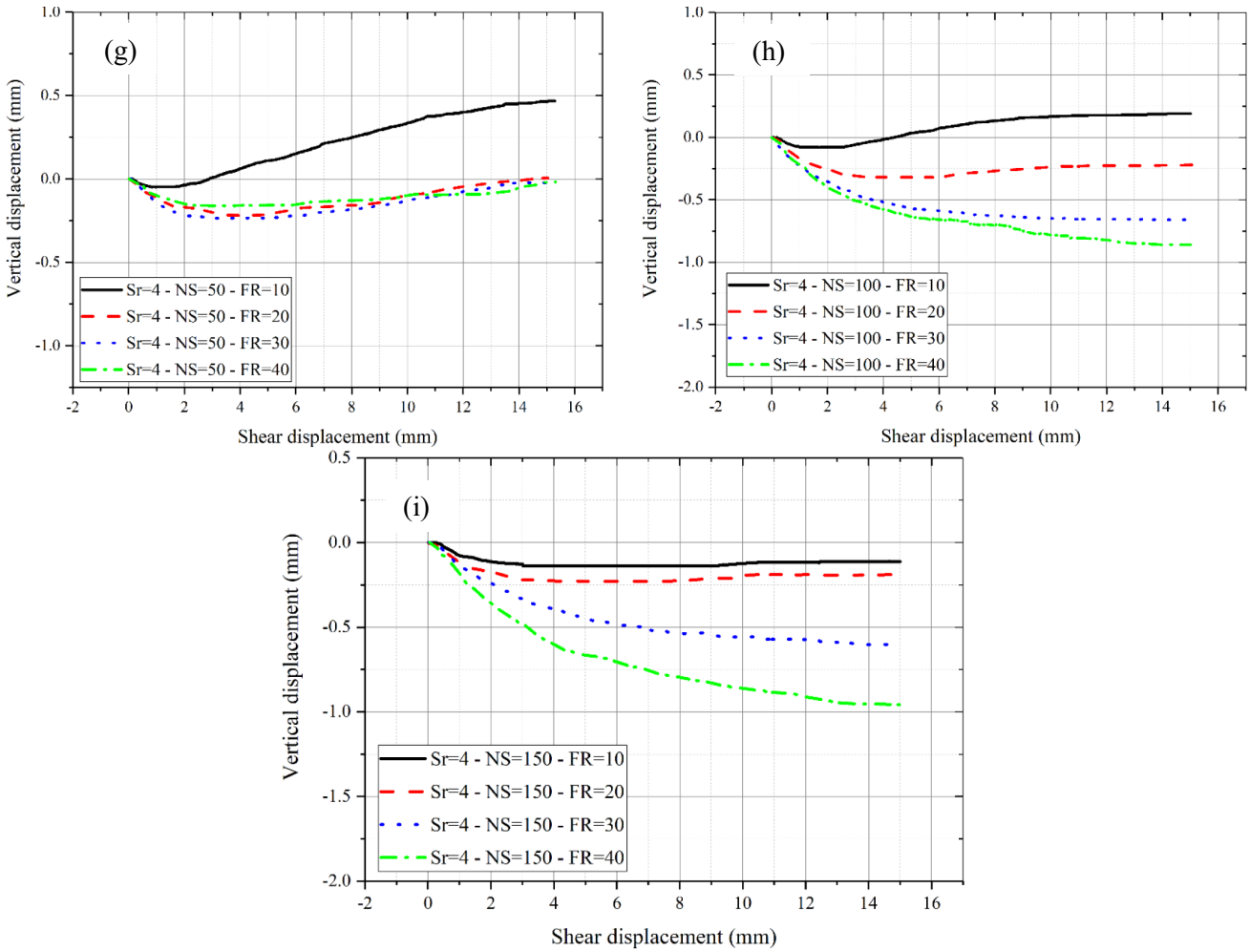


**Fig. 11** (continued)

materials, providing valuable insights into their mechanical behaviour.

## Limitations and future studies

While this paper provides valuable insights into the mechanical behaviour of SRM, there are certain limitations and paths for future research that should be acknowledged. The study primarily focused on a specific soil type with a void ratio of 0.86, which may not fully represent the diverse range of soils encountered in real-world applications. Different soil types, with varying compositions, grain size distributions, and densities, could significantly impact SRM behaviour, warranting further research into SRM performance across various soil conditions. Additionally, the behaviour of SRM under different environmental conditions, such as varying temperatures and moisture levels, remains unexplored and requires investigation to assess its suitability for broader applications. The study's focus on short-term mechanical behaviour also suggests the need for extended laboratory testing and field studies to evaluate the long-term stability and durability of SRM in practical scenarios. Moreover, while SRM presents a promising sustainable geotechnical material, future research should explore its environmental and economic implications, including life cycle assessments and cost-effectiveness compared to traditional materials. Standardization in testing protocols and design guidelines for SRM is essential to ensure consistency in research and practical applications. Beyond traditional geotechnical uses, exploring innovative applications of SRM, such as in sound barriers, pavements, or earthquake-resistant structures, could further enhance its utility. Lastly, the efficiency and environmental impact of processing discarded tires into rubber particles for SRM production need to be optimized, considering the availability and sourcing of these materials. Addressing these limitations and pursuing these research avenues will contribute to a more comprehensive understanding and

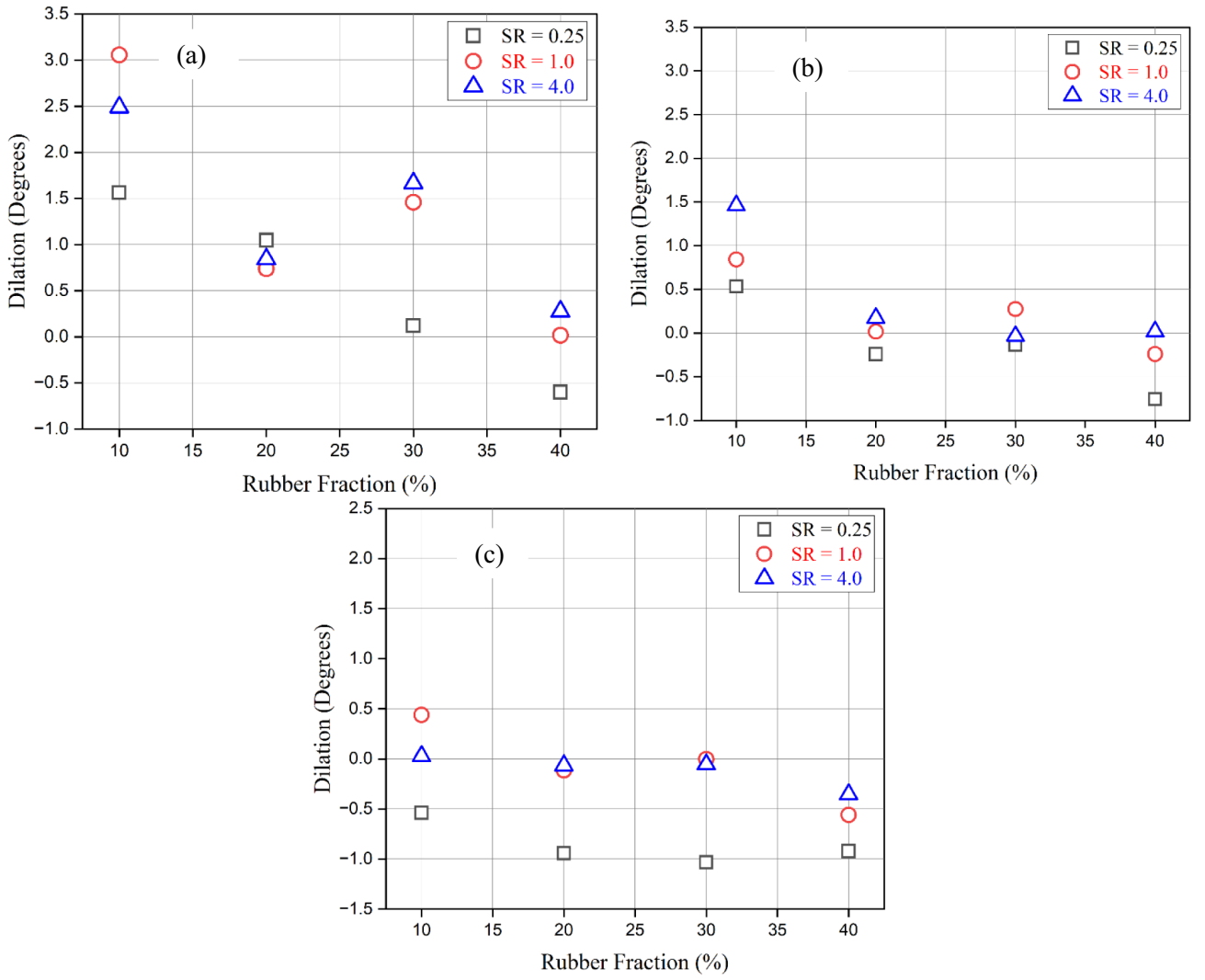


**Fig. 12** Influence of rubber content on the dilatancy of mixtures under NS of: **a** 50 kPa; **b** 100 kPa; and **c** 150 kPa

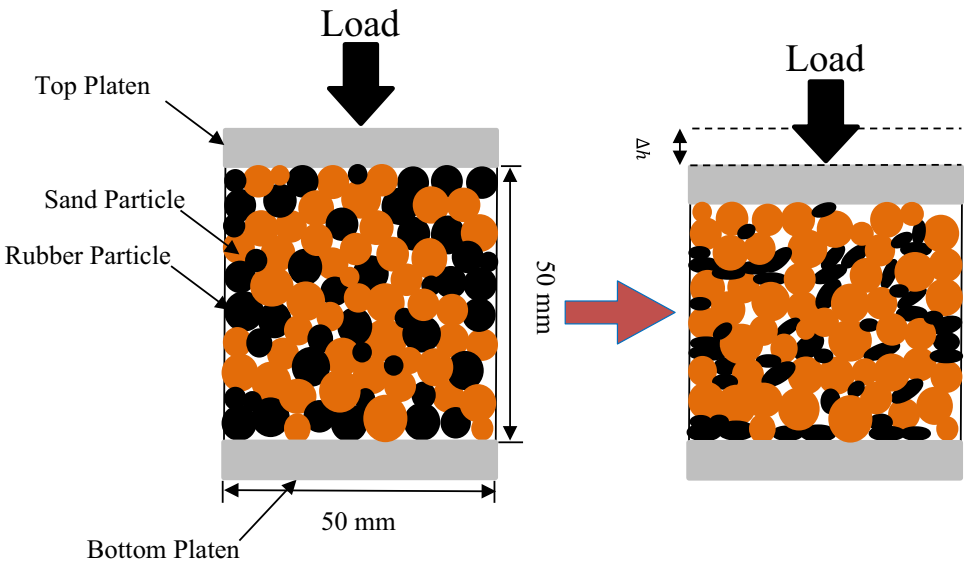


**Fig. 13** Oedometer test with SRM

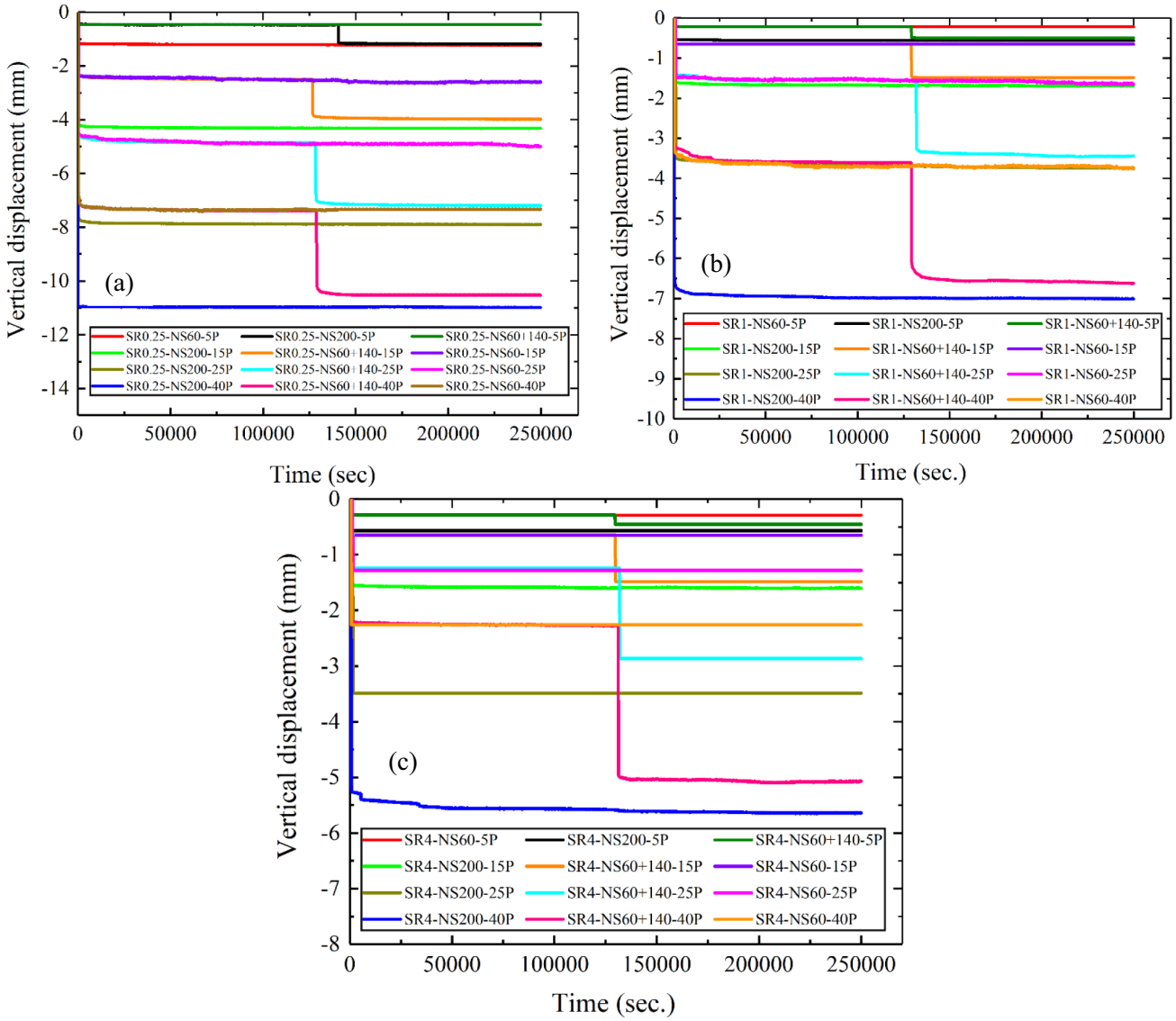


**Fig. 14** Vertical displacement versus time of SRM under different NS for: **a** $SR = 0.25$; **b** $SR = 1$; and **c** $SR = 4$

broader application of SRM in sustainable construction practices.

## Conclusion

Studying mechanical behaviour of SRM, is a critical area of research with implications for geotechnical engineering and construction industries. Understanding how the addition of rubber particles influences deformation, shear strength, and friction angles in these mixtures provides valuable insights for designing sustainable and resilient infrastructure.

The investigation of SRM's mechanical behaviour was the main goal of this work. A wide range of combinations with unique SR of 0.25, 1, and 4 were examined under varied NS of 50, 100, and 150 kPa in a thorough series of studies. The rubber content within the mixtures spanned a wide range, including values of 0%, 5%, 10%, 15%, 20%, 25%, 30%, 40%, and 50%. Additionally, oedometer tests were performed, involving three different SR and three distinct NS conditions: 60 kPa (over a period of three days), 60 + 140 kPa (distributed as 1.5 days followed by another 1.5 days), and 200 kPa (for a total duration of three days). The study's findings can help engineers better understand these materials, for instance, in situations where they are utilized as backfills with little to no compaction.

The results from both the direct shear and oedometer tests have yielded important insights into the mechanical response of SRM. Key findings include:

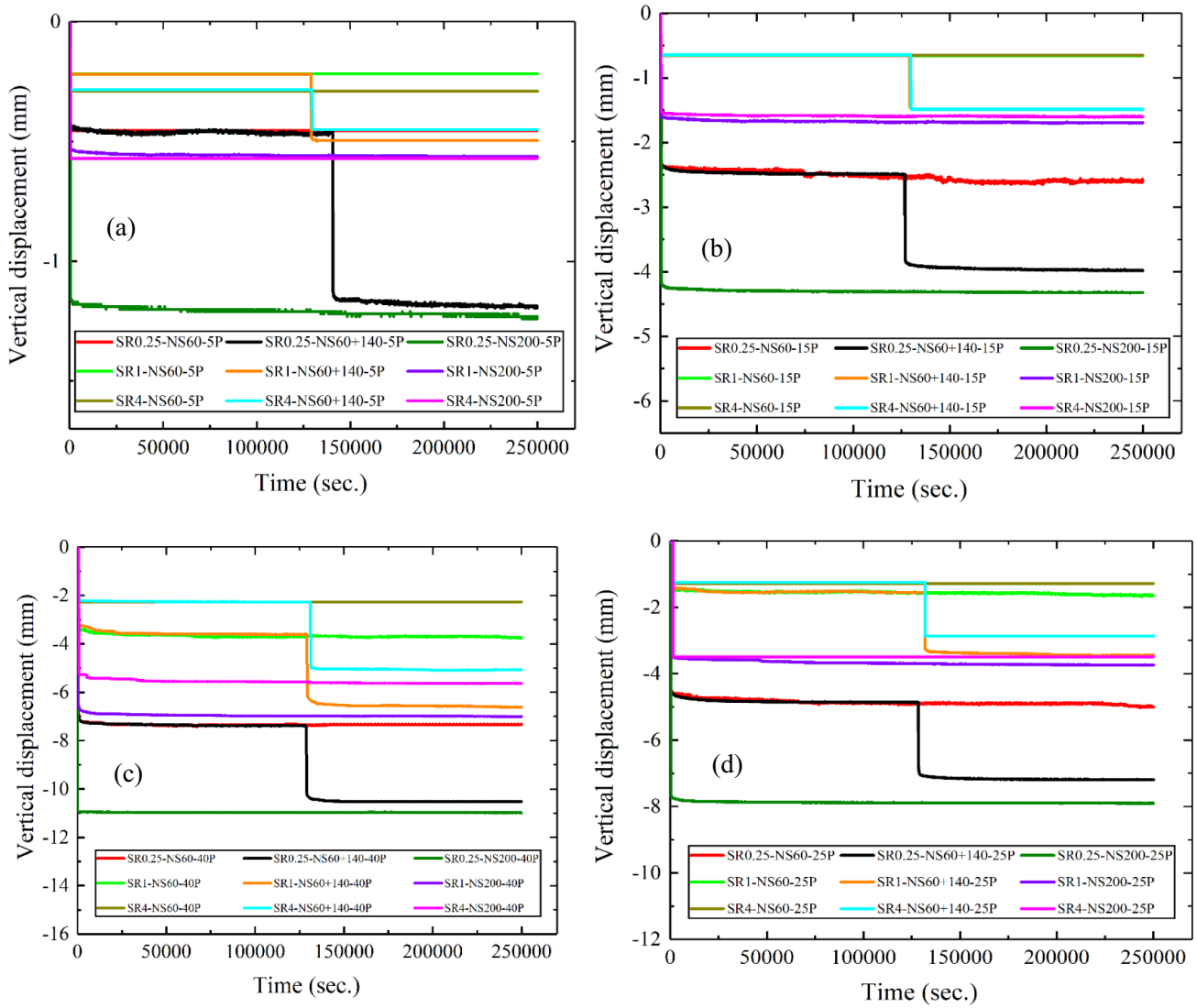


**Fig. 15** Vertical displacement versus time of SRM under different NS for **a** FR = 5 percent; **b** FR = 15 percent; **c** FR = 25 percent; and **d** FR = 40 percent

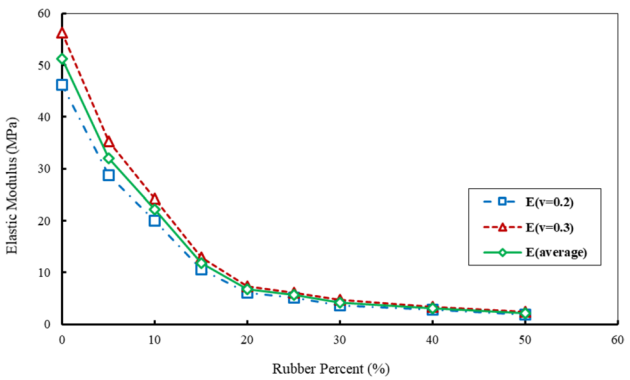


**Fig. 16** Elastic modulus versus rubber percent

1. The shear stress and deformation behaviour of the SRM are notably influenced by the proportions of rubber and the ratio of rubber particle size to sand particle size. The presence of rubber in the mixtures imparts greater deformability to the material, altering its softening behaviour.
2. The internal friction angle of the mixtures exhibits a distinct pattern. It increases significantly with the incorporation of rubber, particularly up to a rubber fraction of 20%. However, a further increase in rubber content has a detrimental effect on the material's friction angle.
3. Depending on the rubber to sand size ratio, the material's shear strength changes. Mixtures with ratios of 1 and 4 exhibit higher shear strength compared to those with a ratio of 0.25.

4. The vertical displacement data analysis of SRM indicates reduced dilation as rubber content increases, especially when exceeding 20%. Dilation behaviour of SRM demonstrated that mixtures with lower SR (SR = 0.25) have lower dilation angles compare to the mixtures with higher SR (SR = 1 and 4).
5. The results showed that the dilation angle depends not only on the content of rubber in the SRM but also on the SR. SRMs with smaller rubber particles exhibited a smaller dilation angle compared to those with the same rubber content but larger SR.
6. Oedometer test results reveal that SRM with an SR of 0.25 exhibit greater deformability and flexibility. Additionally, the addition of more rubber to SRM leads to a reduction in the elastic modulus of the composites.

**Funding** Open Access funding enabled and organized by CAUL and its Member Institutions.

## Declarations

**Competing interest** The authors declare that they have no known competing financial interests or personal relationships that could have appeared to influence the work reported in this paper.



## References

1. Lee J-S, Dodds J, Santamarina JC (2007) Behavior of rigid-soft particle mixtures. J Mater Civ Eng 19(2):179–184
2. Li W et al (2019) Sand type effect on the behaviour of sand-granulated rubber mixtures: integrated study from micro-to macro-scales. Powder Technol 342:907–916
3. Rouhanifar S et al (2021) Strength and deformation behaviour of sand–rubber mixture. Int J Geotech Eng 15(9):1078–1092
4. Fareghian M, Afrazi M, Fakhimi A (2023) Soil reinforcement by waste tire textile fibers: small-scale experimental tests. J Mater Civ Eng 35(2):04022402
5. Hosseini S et al (2023) Prediction of ground vibration due to mine blasting in a surface lead–zinc mine using machine learning ensemble techniques. Sci Rep 13(1):6591
6. Shariati M et al (2024) A state of the art review on geotechnical reinforcement with end life tires. Glob J Environ Sci Manag 10(1):385–404
7. Abdellatief M et al (2024) Physico-mechanical, thermal insulation properties, and microstructure of geopolymer foam concrete containing sawdust ash and egg shell. J Build Eng 90:109374
8. Abdellatief M et al (2023) Production and optimization of sustainable cement brick incorporating clay brick wastes using response surface method. Ceram Int 49(6):9395–9411
9. Afrazi M, Jahed Armaghani D, Afrazi H, Fattahi H, Samui P (2025) Real-time monitoring of tunnel structures using digital twin and artificial intelligence: a short overview. Deep Undergr Sci Eng. https://doi.org/10.1002/dug2.70029
10. Ehsani M, Shariatmadari N, Mirhosseini SM (2017) Experimental study on behavior of soil-waste tire mixtures. Sci Iran 24(1):65–71
11. Tian Y, Senetakis K (2022) Influence of creep on the small-strain stiffness of sand–rubber mixtures. Geotechnique 72(10):899–910
12. Veena U, James N (2023) Natural rubber latex treatment of sand: a novel remediation technique for soil liquefaction. Soil Dyn Earthq Eng 165:107661
13. Badarayani P et al (2023) Sand rubber mixtures under oedometric loading: sand-like vs. rubber-like behavior. Appl Sci 13(6):3867
14. Pérez SPM et al (2024) Effect of crumb rubber and steel slag on asphalt mixtures for a micropavement. Innov Infrastruct Solut 9(2):37
15. Dalvand A, Ahmadi M (2021) Impact failure mechanism and mechanical characteristics of steel fiber reinforced self-compacting cementitious composites containing silica fume. Eng Sci Technol Int J 24(3):736–748
16. Ngo AT, Valdes JR (2007) Creep of sand–rubber mixtures. J Mater Civ Eng 19(12):1101–1105
17. Hasanipanah M et al (2018) Prediction of an environmental issue of mine blasting: an imperialistic competitive algorithm-based fuzzy system. Int J Environ Sci Technol 15:551–560
18. Faradonbeh RS et al (2018) Development of GP and GEP models to estimate an environmental issue induced by blasting operation. Environ Monit Assess 190:1–15
19. Fu R et al (2023) A micromechanical investigation of sand–rubber mixtures using the discrete element method. Eng Geol 318:107106
20. Bandyopadhyay TS, Chakrabortty P, Hegde A (2023) Interaction between geogrid and sand-crumb rubber mixtures in laboratory pullout conditions. Innov Infrastruct Solut 8(5):141
21. Tahwia AM et al (2024) Experimental investigation of rubberized concrete slab-on-grade containing tire-recycled steel fibers. Innov Infrastruct Solut 9(2):46
22. Eldin NN, Senouci AB (1993) Rubber-tire particles as concrete aggregate. J Mater Civ Eng 5(4):478–496
23. Daghistani F et al (2023) Internal friction angle of cohesionless binary mixture sand-granular rubber using experimental study and machine learning. Geosciences (Basel) 13(7):197
24. Gabryś K (2023) Experimental research on compressibility characteristics of recycled concrete aggregate: recycled tire waste mixtures. J Mater Cycles Waste Manag 25(4):1966–1977
25. Gordan B et al (2016) A new model for determining slope stability based on seismic motion performance. Soil Mech Found Eng 53(5):344–351
26. Yin T et al (2018) A numerical estimate method of dynamic fracture initiation toughness of rock under high temperature. Eng Fract Mech 204:87–102
27. Valente M et al (2023) Composite alkali-activated materials with waste tire rubber designed for additive manufacturing: an eco-sustainable and energy saving approach. J Mater Res Technol 24:3098–3117
28. Armaghani DJ et al (2020) Hybrid ANN-based techniques in predicting cohesion of sandy-soil combined with fiber. Geomech Eng 20(3):191–205

29. Meddah A, Laoubi H, Bederina M (2020) Effectiveness of using rubber waste as aggregates for improving thermal performance of plaster-based composites. Innov Infrastruct Solut 5(2):61
30. Abdellatief M et al (2023) A state-of-the-art review on geopolymer foam concrete with solid waste materials: components, characteristics, and microstructure. Innov Infrastruct Solut 8(9):230
31. Kolsky H (1949) An investigation of the mechanical properties of materials at very high rates of loading. Proc Phys Soc London, Sect B 62(11):676
32. Davies EDH, Hunter SC (1963) The dynamic compression testing of solids by the method of the split Hopkinson pressure bar. J Mech Phys Solids 11(3):155–179
33. Akbulut S, Arasan S, Kalkan E (2007) Modification of clayey soils using scrap tire rubber and synthetic fibers. Appl Clay Sci 38(1–2):23–32
34. Nie X et al (2009) Dynamic tensile testing of soft materials. Exp Mech 49:451–458
35. Haddad A, Rezazadeh Eidgahee D (2018) Experimental evaluation of mobilized friction angle of sandy soil–rubber mixtures for different loading stress paths. J Transp Infrastruct Eng 4(2):15–28
36. Adamu M et al (2024) Mechanical, microstructural characteristics and sustainability analysis of concrete incorporating date palm ash and eggshell powder as ternary blends cementitious materials. Constr Build Mater 411:134753
37. Lisi RD, Park JK, Stier JC (2004) Mitigating nutrient leaching with a sub-surface drainage layer of granulated tires. Waste Manag 24(8):831–839
38. Jamshidi Chenari R et al (2017) An experimental and numerical investigation into the compressibility and settlement of sand mixed with TDA. Geotech Geol Eng 35:2401–2420
39. Bahadori H et al (2018) A comparative study between gravel and rubber drainage columns for mitigation of liquefaction hazards. J Rock Mech Geotech Eng 10(5):924–934
40. Afrazi M, Yazdani M (2021) Determination of the effect of soil particle size distribution on the shear behavior of sand. J Adv Eng Comput 5(2):125–134
41. Afrazi M et al. (2023) Development and evaluation of a computer-aided educational platform for advancing understanding of slope stability analysis. Civ Eng Infrastruct J 2322
42. Nowroozi V et al (2021) Optimum design for soil nailing to stabilize retaining walls using FLAC3D. J Adv Eng Comput 5(2):108–124
43. Huat CY, Armaghani DJ, Lai SH, Motaghedi H, Asteris PG, Fakharian P (2024) Analyzing surface settlement factors in single and twin tunnels: a review study. J Eng Res. https://doi.org/10.1016/j.jer.2024.05.009
44. Yu Huat C, Jahed Armaghani D, Bin Hashim H, Fattahi H, He X, Asteris PG, et al. (2025) Development of a practical solution to predict surface settlement induced by twin tunnels. J Struct Des Constr Pract 30(1):04024097. https://doi.org/10.1061/JSDCCC.SCENG-1614
45. Dai B-B et al (2023) A reinterpretation of the mechanical behavior of rubber–sand mixtures in direct shear testing. Constr Build Mater 363:129771
46. Wu M et al (2023) Dynamic behavior of geocell-reinforced rubber sand mixtures under cyclic simple shear loading. Soil Dyn Earthq Eng 164:107595
47. Zhang J-Q, Wang X, Yin Z-Y (2023) DEM-based study on the mechanical behaviors of sand–rubber mixture in critical state. Constr Build Mater 370:130603
48. Zhou J et al (2023) Chart-based granular slope stability assessment using the modified Mohr-Coulomb criterion. Arab J Sci Eng 48(4):5549–5569
49. Mei X et al (2023) Development of a hybrid artificial intelligence model to predict the uniaxial compressive strength of a new aseismic layer made of rubber–sand concrete. Mech Adv Mater Struct 30(11):2185–2202
50. Bunawan AR et al (2018) Experimental and intelligent techniques to estimate bearing capacity of cohesive soft soils reinforced with soil-cement columns. Measurement 124:529–538
51. Tsang L, Akbari M, Fakharian P (2025) Prediction of soil liquefaction using a multi-algorithm technique: stacking ensemble techniques and bayesian optimization. J Soft Comput Civ Eng 9(2):33–56. https://doi.org/10.22115/scce.2024.453006.1860
52. Ye X, Moayedi H, Khari M, Foong LK (2020) Metaheuristic-hybridized multilayer perceptron in slope stability analysis. Smart Struct Syst Int J 26(3):263–275
53. Kawata S et al. (2007) Undrained and drained shear behavior of sand and tire chips composite material
54. Garga VK, O'Shaughnessy V (2000) Tire-reinforced earthfill. Part 1: construction of a test fill, performance, and retaining wall design. Can Geotech J 37(1):75–96
55. O'Shaughnessy V, Garga VK (2000) Tire-reinforced earthfill. Part 2: pull-out behaviour and reinforced slope design. Can Geotech J 37(1):97–116
56. Poh PSH, Broms BB (1995) Slope stabilization using old rubber tires and geotextiles. J Perform Constr Facil 9(1):76–79
57. Huat BBK, Aziz AA, Chuan LW (2008) Application of scrap tires as earth reinforcement for repair of tropical residual soil slope. Electron J Geotech Eng 13:1–9
58. Wu WY, Benda CC, Cauley RF (1997) Triaxial determination of shear strength of tire chips. J Geotech Geoenviron Eng 123(5):479–482
59. Ghazavi M, Sakhi MA (2005) Influence of optimized tire shreds on shear strength parameters of sand. Int J Geomech 5(1):58–65
60. Mucsi G, Szenczi Á, Nagy S (2018) Fiber reinforced geopolymer from synergetic utilization of fly ash and waste tire. J Clean Prod 178:429–440
61. Yang Z et al (2020) Advances in properties of rubber reinforced soil. Adv Civil Eng 2020:1–16
62. Zrar YJ, Younis KH (2022) Mechanical and durability properties of self-compacted concrete incorporating waste crumb rubber as sand replacement: a review. Sustainability 14(18):11301
63. Masad E et al (1996) Engineering properties of tire/soil mixtures as a lightweight fill material. Geotech Test J 19(3):297–304
64. Zornberg JG, Cabral AR, Viratjandr C (2004) Behaviour of tire shred sand mixtures. Can Geotech J 41(2):227–241
65. Bergado DT, Youwai S, Rittirong A (2005) Strength and deformation characteristics of flat and cubical rubber tyre chip–sand mixtures. Geotechnique 55(8):603–606
66. Jamshidi Chenari R, Alaie R, Fatahi B (2019) Constrained compression models for tire-derived aggregate-sand mixtures using enhanced large scale oedometer testing apparatus. Geotech Geol Eng 37:2591–2610
67. Youwai S, Bergado DT (2003) Strength and deformation characteristics of shredded rubber tire sand mixtures. Can Geotech J 40(2):254–264
68. Takano D, Chevalier B, Otani J (2014) Experimental and numerical simulation of shear behavior on sand and tire chips
69. Liu F-Y, Li H-Z, Sun H-L (2023) Effect of rubber–sand particle size ratio on shear properties of rubber–sand mixtures under normal cyclic loading. Constr Build Mater 406:133415
70. Boominathan A, Banerjee S (2021) Engineering properties of sand–rubber tire shred mixtures. Int J Geotech Eng. https://doi.org/10.1080/19386362.2019.1617479
71. Rezamand A, Afrazi M, Shahidikhah M (2021) Study of convex corners' effect on the displacements induced by soil-nailed excavations. J Adv Eng Comput 5(4):277–290
72. Taghizadeh K et al (2023) X-ray 3D imaging-based microunderstanding of granular mixtures: stiffness enhancement by

adding small fractions of soft particles. Proc Natl Acad Sci USA 120(26):e2219999120
73. Won J, Ryu B, Choo H (2023) Evolution of maximum shear modulus and compression index of rigid–soft mixtures under repetitive K 0 loading conditions. Acta Geotech. https://doi.org/10.1007/s11440-023-01945-x
74. Akbarimehr D et al (2023) Deformation characteristics of rubber waste powder–clay mixtures. Sustainability 15(16):12384
75. Yeo JY, Kim SY, Lee J-S (2023) Compressibility and small strain stiffness characteristics of silt-hematite mixtures. Eng Geol 325:107282
76. Neaz Sheikh M et al (2013) Shear and compressibility behavior of sand–tire crumb mixtures. J Mater Civ Eng 25(10):1366–1374
77. Rouhanifar S, Ibraim E (2015) Mechanics of soft–rigid soil mixtures
78. Naderpour H, Mirrashid M (2020) Evaluation and verification of finite element analytical models in reinforced concrete members. Iran J Sci Technol Trans Civ Eng 44(2):463–480
79. Naderpour H, Mirrashid M (2019) A Neuro-fuzzy model for punching shear prediction of slab-column connections reinforced with FRP. J Soft Comput Civ Eng 3(1):16–26
80. Fareghian M, Afrazi M, Jahed Armaghani D, Akhoundan M, Asghari N, Yazdani M (2026) Machine learning in the modeling of 3D printed soil-cement materials: a short overview. J Soft Comput Civ Eng 10(2):1966. https://doi.org/10.22115/scce.2025.1966
81. Holownia BP (1972) Effect of Poisson's ratio on bonded rubber blocks. J Strain Anal 7(3):236–242
82. Rouhanifar S, Afrazi M (2019) Experimental study on mechanical behavior of sand–rubber mixtures
83. Liu L, Cai G, Liu S (2018) Compression properties and micromechanisms of rubber–sand particle mixtures considering grain breakage. Constr Build Mater 187:1061–1072
84. Evans TM, Valdes JR (2011) The microstructure of particulate mixtures in one-dimensional compression: numerical studies. Granul Matter 13:657–669
85. Perez JCL, Kwok CY, Senetakis K (2017) Micromechanical analyses of the effect of rubber size and content on sand–rubber mixtures at the critical state. Geotextiles Geomembr 45(2):81–97
86. Vermeer PA, De Borst R (1984) Non-associated plasticity for soils, concrete and rock. HERON 29(3):0046–7316
87. Anvari SM, Shooshpasha I, Kutanaei SS (2017) Effect of granulated rubber on shear strength of fine-grained sand. J Rock Mech Geotech Eng 9(5):936–944
88. Al-Bared MAM et al (2021) Application of hybrid intelligent systems in predicting the unconfined compressive strength of clay material mixed with recycled additive. Transp Geotech 30:100627
89. Mistry MK, Shukla SJ, Solanki CH (2021) Reuse of waste tyre products as a soil reinforcing material: a critical review. Environ Sci Pollut Res 28(20):24940–24971
90. Behzadian A, Oliae M (2015) Dilation behavior analysis of the interaction region between a nail and the soil in the case of pull-out. In: Second national conference on civil engineering, architecture, and urban development